*Quest Journals*
*Journal of Research in Environmental and Earth Sciences*
*Volume 6 ~ Issue 4 (2020) pp: 34-47*
*ISSN(Online) :2348-2532*
www.questjournals.org

**Research Paper**

# Efficiency of a biosorbent from *Aegle marmelos* leaves for removal of MB and BG from aqueous solution using column method

Smita Baruah
*Assam Down Town University, Department of Chemistry, Panikhaiti, Guwahati, Assam*

***ABSTRACT:*** *The indigenously prepared low-cost Aegle Marmelos leaves powder (AMLP) showed great potential for removing Methylene Blue (MB) and Brilliant Green (BG) from aqueous solution in single dye system. The influence of various experimental factors bed depths, feed concentrations and flow rate were investigated. The adsorption capacities at 90 % and 50 % breakthrough points increased from 2.30 to 3.55 mgg$^{-1}$ and 1.15 to 2.90 mgg$^{-1}$ for MB and 2.85 to 2.99 mgg$^{-1}$ and 1.24 to 2.90 mgg$^{-1}$ for BG with increase in bed height from 1.4 cm to 2.4 cm and 2.61 to 5.10 mg g$^{-1}$ and 1.37 to 3.48 mg g$^{-1}$ for MB and 1.25 to 3.90 mg g$^{-1}$ and 2.38 to 5.20 mgg$^{-1}$for BG with increase in feed concentrations from 10 to 30 mgL$^{-1}$ respectively. However, with increase in flow rate adsorption capacities on CAMLP for 90 % breakthrough decreases from 4.49 to 2.75 mg g$^{-1}$ for MB and 5.57 to 2.42 mg g$^{-1}$ for BG and for 50% breakthrough it decreases from 3.57 to 0.92 mg g$^{-1}$ for MB and 3.71 to 1.68 mgg$^{-1}$ for BG respectively. The Bohart- Adam's model was also fitted with the adsorption data for both MB and BG on CAMLP.*

***Keywords:*** *Aegle Marmelos, Leaf Powder, Methylene Blue, Brilliant Green, Column, Breakthrough, Bohart-Adam's Model.*

*Received 24 November, 2020; Accepted 08 December, 2020 © The author(s) 2020.*
*Published with open access at www.questjournals.org*

## I. INTRODUCTION

The day to day human activities and industrial revolution have influenced the flow and storage of water and the quality of available fresh water dyes are widely used in industries such as textile, rubber, paper, plastic cosmetic etc. Among these various industries, textiles ranks first in usage of dyes for coloration of fibre. Colour removal from textile effluents has been the subject of great attention not only because of its toxicity but mainly due to its visibility. Through hundred of years, the scale of production and the nature of dyes have changed drastically, consequently the negative impact of dyes on the environment has increased.

Therefore it is our responsibility for the treatment of dyes to eliminate any impact on human health. However colored wastewater is treated by physico-chemical processes[1]. But due to the formation of toxic by-products and intensive energy requirements[2] these treatments are ineffective in removing dyes, expensive and are not applicable to a wide range of colored water [3].

Therefore, decolourisation has been the subject of research in recent years. Dye removal is a complex and expensive process. The most widely used methods for removal of dyes from wastewater include ion-exchange, chemical and electrochemical oxidation, membrane processes, coagulation-flocculation, and adsorptions [4]. Most of these methods suffer from some drawbacks, such as high capital and operational cost or the disposal of the residual sludge and are not suitable for small scale industries.

Therefore, three different processes such as biosorption, biodegradation and bioaccumulation are considered to be most effective methods for dye removal from wastewater [5]. The biosorption is considered the most advantageous than others for the treatment of colored waters [6] and is identified as the preferred technique for decolorization by giving the best results [7].

Biosorption plays an important role in removal of dyes from aqueous solution in water pollution control. The main advantages of this technique are the reusability of biomaterial, low operating cost, short operation time and no production of secondary compounds that might be toxic.

The objectives of the present work are to investigate the biosorption potential of AMLP biomass for the removal of MB and BG from aqueous solution using column method. Optimum biosorption conditions were determined as a function of bed depth, flow rate and initial feed concentration.

## II. MATERIALS AND METHODS

### 2.1. Collection and Preparation of biosorbent

Mature *Aegle marmelos* leaves were collected from Morigaon district of Assam (India) and washed with fresh water for several times to remove sand, dirt and epiphytes. After drying dried at 373-383 K for 3 – 5 hours in hot air oven, the dried leaves were crushed into powder in a mechanical grinder to obtain the *Aegle marmelos* leaves powder (AMLP). The biosorbent was obtained by washing the same repeatedly with water to remove soluble materials, dyes and pigments and finally drying at 373-383 K for 4hrs in an air oven. The dried AMLP was sieved and the 100-200 mesh fraction was separated. The separated AMLP was preserved in plastic sealed packed for further use as an adsorbent.

### 2.2. Preparation of Clay Bound biosorbent

The granules for column study were prepared by mixing the biosorbent powder with locally available pottery clay as a binder in the weight ratio of 9:1 (9 g clay, 1.0 g biosorbent powder) and converting the same into a uniform paste by adding a few drops of double-distilled water. The paste was drawn into long granules through a syringe of internal diameter of 1.5 mm, cut into small granules, dried in an air oven at 60°C -70°C for 2-3 h followed by burning of the dried granules over a gas burner. The burned granulated forms of clay bound biosorbents were kept in desiccators for further use Plate 1.

### 2.3. Preparation of standards solution of Methylene Blue (MB) and Brilliant Green (BG)

Stock solution of MB and BG were prepared by dissolving 1gm of dye in 1000 ml of de-ionised, double distilled water. Required initial concentration of MB and BG samples were prepared by appropriate dilution of the above stock standards solutions. A Standard calibration curve were drawn by measuring the absorbance at $\lambda_{max}$ 665nm for MB and $\lambda_{max}$ 625nm for BG spectrophotometrically (Beckmann Coulter 700).

**Plate 1.** Granules of clay bound *Aegle marmelos* leaf powder (CAMLP)

### 2.3. Instrument analysis

The FTIR spectra of AMLP was obtained with a with a Perkin Elmer spectrometer (Model Spectrum RX I) using 'nujol' method for sample introduction. The AMLP samples were kept in an oven at 333–343 K overnight for getting rid of moisture, allowed to cool to room temperature in a desiccator and then, a tiny amount was spread on a nujol film between two KBr windows.

The surface morphologies of AMLP was observed directly with a scanning electron microscope (Type Carl-Zeiss,Σigma-VP).

Energy dispersive X-ray spectroscopy (EDS) was also carried out using Energy dispersive X-ray analysis (EDX) INCA 4.15 EDS software (Oxford Instruments).

The pH of the AMLP was determined in a 10% slurry (10 g powder in 100 mL double distilled water) with a digital pH-meter (ELICO LI-10).

The average specific surface area of the powder was determined with the methylene blue adsorption method [8].

### 2.4. The dynamic column studies

The adsorption experiments were performed in column mode. The concept of the breakthrough curve is used to describe the performance of a fixed bed column. In the present study, the fixed bed column study for both methylene blue (MB) and brilliant green (BG) removal from aqueous solution by clay bound biosorbents

granules i.e. CAMLP was conducted by using a pyrex glass tube having inner diameter of 2.9 cm and 30 cm height. The column was packed with CAMLP granules between two layers of glass wool. The bed is rinsed with distilled water and left overnight to ensure a closed packed arrangement of adsorbent granules without any kinds of voids, channels or cracks. The column was then fed continuously with dye solution of desired concentration maintaining a constant flow rate throughout the experiment. The effluent samples were collected at a predetermined volume interval of 25 mL in 100 mL conical flask and the remaining dye concentration was monitored spectrophotometrically using a spectrophotometer (Beckmann Coulter 700) at $\lambda_{max}$ 665 nm for MB and 625 nm for BG respectively.

**Table 1-** Experimental conditions for the dynamic column studies

| | **Column adsorption** | |
|---|---|---|
| 1 | Bed Depth or Bed height (cm) | 1.4, 1.9, 2.4 |
| 2 | Flow Rate($mLmin^{-1}$) | 1.5, 3.7, 5.2 |
| 3 | Feed concentration Dye ($mgL^{-1}$) | 10, 20, 30 |

**2.5. Fixed bed column studies**

The Column adsorption operation, Weber 1972 [9] creates a continuous concentration gradient where an adsorbate solution of constant concentration is allowed to flow continuously through a fixed bed of the adsorbent solid. In the column operation as the adsorption continues, the concentration of the adsorbate solution in contact with the fixed adsorbent layer is relatively constant. The efficiency of column operations is described by the breakthrough curves which is obtained by plotting $C_t/C_o$ ($C_t$ concentration of the adsorbate solute in the eluent, $C_o$ is the initial concentration of the influent which enters the column) against time of treatment (t) or bed volume (BV) treated. The time for breakthrough appearance and the shape of the breakthrough curves are very important characteristics for determining the operation and the dynamic response of an adsorption column. The characteristic shape of the breakthrough curve depends on the balance between the solid phase of the fixed bed column and the liquid phase of the feed aqueous adsorbate, based on the kinetic adsorption processes such as diffusion in the bulk fluid, external mass transfer, inter-particle mass transfer and micropore adsorption [10].
The breakthrough curve exhibits a characteristic "S" shape but varies considerably in degree of steepness for different situation (Weber, 1972). Some of the important features of the breakthrough curves are breakthrough capacity, exhaustion capacity, degree of column utilization (DOC) and mass transfer zone (MTZ) [11].
(a) The mass of adsorbate eliminated by the unit mass of adsorbent bed at breakthrough time or breakthrough concentration is termed as the breakthrough capacity. It is expressed as:

$$q_{bc} = \frac{(C_o - C_b)V_b}{m} \qquad (1)$$

where,

$q_{bc}$ = Breakthrough capacity ($mg\ g^{-1}$)
$C_o$= Initial concentration of the influent ($g\ L^{-1}$)
$C_b$= Concentration of the effluent at the breakthrough point ($g\ L^{-1}$)
$V_b$ = Volume of the effluent (ml)
m = Mass of sorbents (g)

(b) The mass of the adsorbate removed by unit mass of the fixed adsorbent at saturation point (i.e. inlet concentration of the influent ($C_0$) is almost equal to the outlet concentration of the effluent ($C_t$), $C_o \sim C_t$) is known as the exhaustion or saturation capacity.

$$q_{sc} = \frac{(C_o - C_s)V_s}{m} \qquad (2)$$

where,

$q_{sc}$ = Saturation capacity ($mg\ g^{-1}$)
$C_o$= Initial concentration of the influent ($g\ L^{-1}$)
$C_s$= Concentration of the effluent at the saturation point ($g\ L^{-1}$)
$V_s$= Volume of the effluent (ml)
m = Mass of sorbents (g)

(c) The mass adsorbed at breakthrough point divided by the mass adsorbed at complete saturation point is defined as the degree of column utilization (DOC).

$$DOC = \frac{V_b}{V_s} \quad (3)$$

where,

D= degree of column utilization
$V_b$= Volume of solute solution adsorbed at breakthrough point (ml)
$V_s$= Volume of solute solution adsorbed at saturation point (ml)

(d) The mass transfer zone (MTZ) is defined as the active adsorption zone in a packed column where active adsorption occurs.

$$MTZ = H(1 - \frac{t_b}{t_s}) \quad (4)$$

where,

H = Height of sorbent bed (cm)
$t_b$ = Breakthrough time(min)
$t_s$ = Saturation time (min)

The adsorption behaviour of solute solution in a fixed bed column is expressed in terms of $C_t/C_o$ with respect to time for a given bed depth, flow rate and initial solute concentration, which consequently gives a breakthrough curve.

**2.6 Bohart-Adam's model**

A successful design of a column adsorption process requires a description of the dynamic behaviour of adsorbate in a fixed bed. The dynamic behaviour of a solute in a fixed bed under defined operating conditions is difficult to predict because the process does not occur at a steady state, while the influent still passes through the bed. Uneven flow pattern throughout the column usually results in an incomplete exhaustion of the bed. The Bed Depth Service Time (BDST) model also known as Bohart-Adam's model (Bohart and Adam, 1920) describes the initial part of the breakthrough curve. The Bohart- Adam's model is mainly based on the surface reaction theory and it assumed that the rate of adsorption is proportional to fraction of adsorption capacity on the adsorbent [12]. The expression of the model is given below

$$t = \frac{N_0 D}{C_0 \nu} - \frac{1}{K_{AB} C_0} \ln(\frac{C_0}{C_t} - 1) \quad (5)$$

Where,
$K_{AB}$ = kinetic constant ($Lmg^{-1}min^{-1}$),
$\nu$ = linear velocity calculated by dividing the flow rate by the column section area ($cmmin^{-1}$),
D = bed depth of column (cm),
$N_o$ = adsorption capacity per unit volume of bed in ($mg\ L^{-1}$),
$C_o$ = initial concentration of the influent in ($mg\ L^{-1}$) and
$C_t$ = effluent concentration in ($mg\ L^{-1}$).
The BDST equation describes how the mass transfer zone progresses through a single fixed bed of adsorbent. For getting accurate results, the required condition is that the MTZ should move through the column at a constant rate and so a constant pattern of MTZ, a constant feed concentration and a constant feed flow rate are required. In the present work, the BDST model is used to describe and predict the dynamic behaviour of the clay-bound biosorbent beds in column performance.

**2.7 Desorption and regeneration study**

A successful desorption process requires an appropriate selection of eluent, which strongly depends on the mechanism of adsorption process and on the type of adsorbent used. Eluent must not damage the biosorbent used and should be cost effective and eco-friendly to the environment. Most of the effective eluents such as very dilute concentration of acids (such as $H_2SO_4$, HCl, HCOOH, $HNO_3$ and $CH_3COOH$), alkalis (such as $NaHCO_3$, $Na_2CO_3$, NaOH, KOH and $K_2CO_3$), salts (such as $(NH_4)_2SO_4$, NaCl, KCl, $KNO_3$, $CaCl_2.2H_2O$, $NH_4NO_3$ and $C_6H_5Na_3O_7.2H_2O$), deionised water, chelating agents and buffer solutions (such as bicarbonate and phosphate)

used in desorption process for effective regeneration and adsorbent recovery of adsorbent were used in various studies.

## III. RESULTS AND DISCUSSION

### 3.1 Characterization of biosorbent

The FTIR spectra (Fig.1) of AMLP indicated the presence of a number of important functional groups which might have been involved in interacting with the dye molecules/ions. The broad band between 3600 and 3000cm$^{-1}$ is characteristic of –OH stretching vibrations showing that AMLP surface has a large number of alcoholic and phenolic –OH groups. The multiple bands from 1700 to 1500cm$^{-1}$ related >CO groups of carboxylic acids, -$NH_2$ groups, N-H bending C-N stretching of primary and secondary amines, and -C=C- groups of alkenes. >CO groups also known to interact with dye molecules [13]. The bands from 1300 to 1000 cm$^{-1}$ attributed to -CO linkages in alcohol, ethers, carboxylic acids, esters etc. The absorption band at 1633-515cm$^{-1}$may be due to the aromatic domain in the plant leaves [14]. Thus the FTIR measurements, clearly indicates that the AMLP surface contains a variety of functional groups, such as –OH, -$NH_2$, NH, -R-SC=O (thioester), -COOH, $R_1$-S(=O=O)-N(-$R_2$, -$R_3$) (sulphonamide), and functional groups involves in binding adsorbate to the adsorbent surface. The FT-IR results clearly indicate that the AMLP has several functional groups which are able to react with positively charged adsorbate molecules in aqueous solution.

In order to study the adsorption behaviour of MB and BG, SEM and EDS were carried out in AMLP before Plate 2 shows the SEM micrographs of AMLP samples before adsorptions of dyes. The surface of AMLP was highly heterogeneous with a large number of steps, boroughs and waves having a completely uneven topography. It is clear that in addition to a heterogeneous surface area, AMLP has considerable number of porous sites that indicates a good possibility for dye to be trapped and adsorbed.

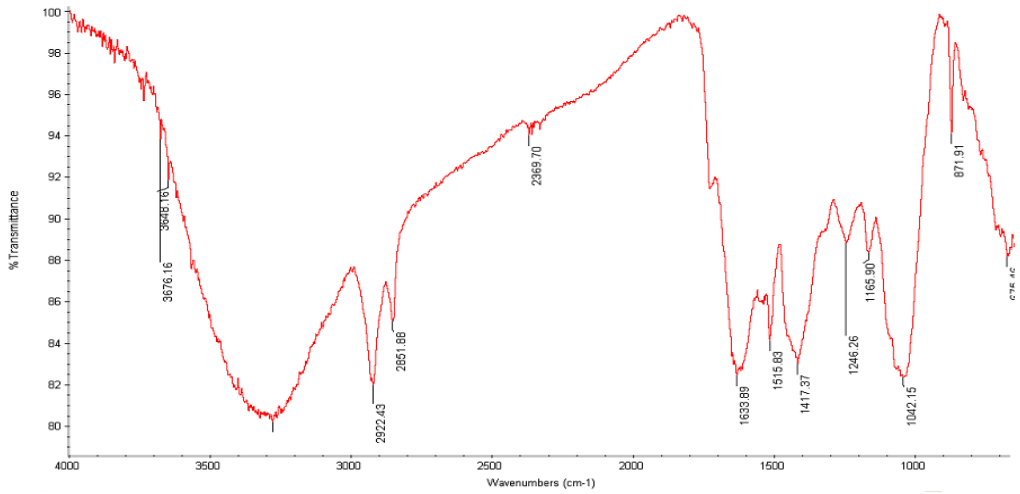


**Figure 1:** FTIR spectra of *Aegle marmelos* leaf powder (AMLP).

Energy dispersive X-ray spectrums (EDS) of AMLP before adsorption of MB and BG is shown in Plate 3. The results of EDS analysis of AMLP before adsorptions showed the presence of the major and minor elements- C, O, Na, Mg, K, Ca, Fe.

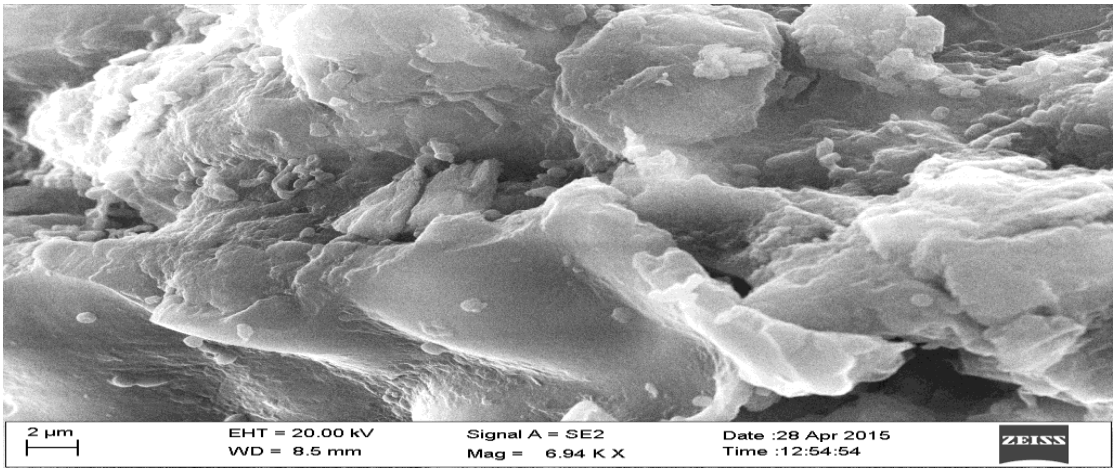


**Plate 2.** SEM micrograph of *Aegle marmelos* leaf powder (AMLP)

The average monolayer capacity for methylene blue adsorption on AMLP was measured as 52.63 mg/g and the cross-sectional area of the dye molecule being $1.30\times10^{-18}m^2$, the specific surface area is 110.21 $m^2g^{-1}$.

### 3.2 The Column Study

#### 3.2.1 Effect of bed depth

The time for breakthrough appearance and the shape of the breakthrough curve are very important characteristics for determining the operation and the dynamic response of an adsorption fixed-bed column [15]. The breakthrough curves are obtained by plotting $C_t/C_o$ ($C_t$ concentration of the adsorbate solute in the eluent, $C_o$ the initial concentration of the influent) against volume of MB and BG solution.

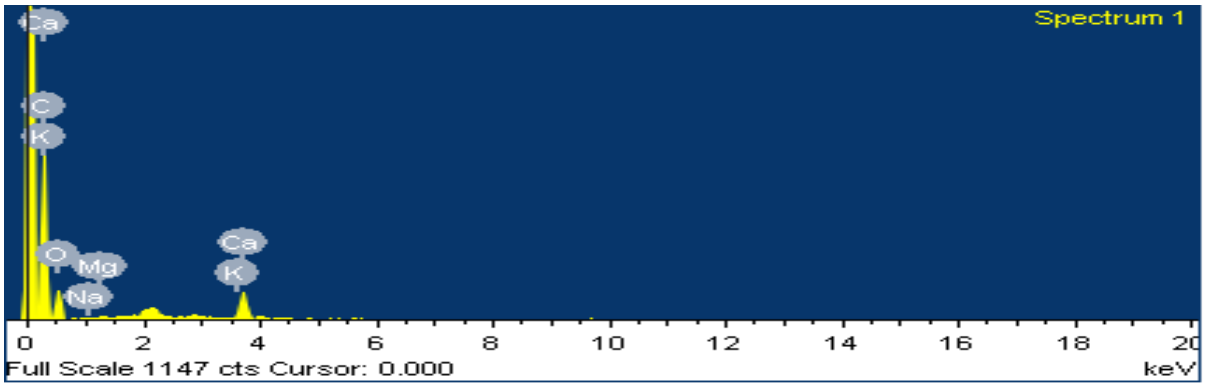


**Plate 3.** Energy Dispersive X-ray spectra (EDX) of *Aegle marmelos* leaf powder (AMLP).

The breakthrough curve for MB and BG sorption at three different bed depths 1.4 cm, 1.9 cm and 2.4 cm, at constant feed concentration (20 mg $L^{-1}$) and flow rate 1.5 $mLmin^{-1}$ are shown in Figure.2 and Figure.3 respectively. The adsorption capacities at 90 % and 50 % breakthrough points for clay bound AMLP (CAMLP) showed an increasing trend for both dyes. At 90 % and 50% break through point for MB, adsorption capacity increased from 2.30 to 3.55 mg $g^{-1}$ and 1.15 to 2.90 mg $g^{-1}$, with increasing bed depth respectively. Similarly, for BG adsorption capacity at 90 % and 50% break through point increases from, 2.85 to 2.99 mg $g^{-1}$ and 1.24 to 2.90 mg $g^{-1}$ respectively with increase in bed height from 1.4 cm to 2.4 cm.

The higher sorption of MB and BG with increasing the bed height is due to an increase in the total surface area of the sorbents, providing more binding sites for MB and BG ions [6]. Although the breakthrough capacities did not show much variation at different bed depths of 1.4 cm, 1.9 cm and 2.4 cm (Table 2) which indicates the consistency and affinity for MB and BG sorption which is an essential factor for the removal of MB and BG by clay bound AMLP sorbents (CAMLP). It was seen from the breakthrough curve that the breakthrough time at 90% breakthrough increases from 11.11 to 27.22 h for MB and 12.78 to 21.11h for BG. Similarly, in case of 50% breakthrough, breakthrough time increases from 5.56 to 22.22 h for MB and 8.33 to 16.11 h for BG with increasing bed height from 1.4 cm, 1.9 cm and 2.4 cm. It may be because of the reason that with the increase in bed height the adsorbate (dye molecules /ions) have more time to contact with the adsorbent bed, the availability of the effective surface area of adsorbent is more which offers more active sites to

adsorption and it also broadens the mass transfer zone length, results in increased breakthrough time as well as adsorption capacity at higher bed height [16] [17].

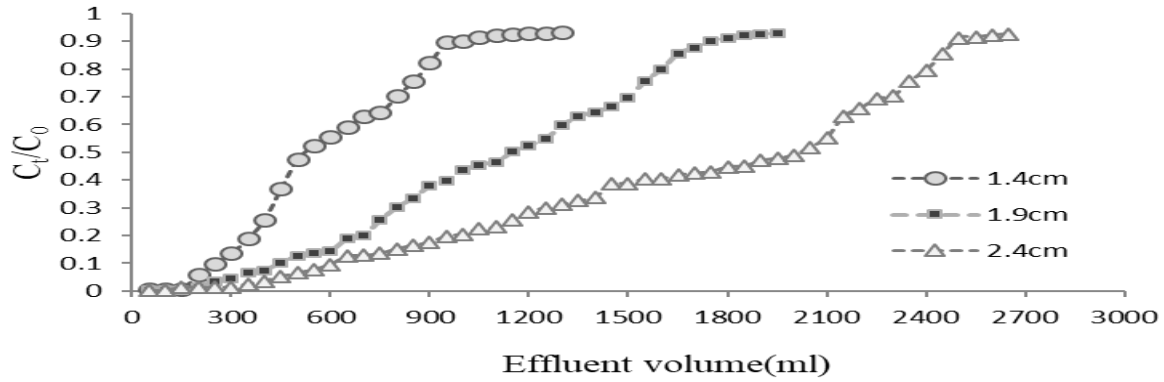


**Figure 2**: Effects of bed depth on adsorption of MB on clay bound AMLP (CAMLP) at 303K (flow rate 1.5 mL $min^{-1}$, MB concentration 20 $mgL^{-1}$).

**3.2.2. Effect of feed concentration of dyes**

The effect of feed concentration of dyes MB and BG on packed column of CAMLP was investigated under column mode with three different initial concentrations of both dyes (10, 20 and 30 mg $L^{-1}$) at bed depth 1.4 cm and flow rate 1.5 mL $min^{-1}$. The breakthrough curve for MB and BG sorption at three different feed concentrations 10, 20 and 30 mg $L^{-1}$, at constant bed depth (1.4 cm) and flow rate 1.5 mL $min^{-1}$ are shown in Figure. 4 and 5 respectively.

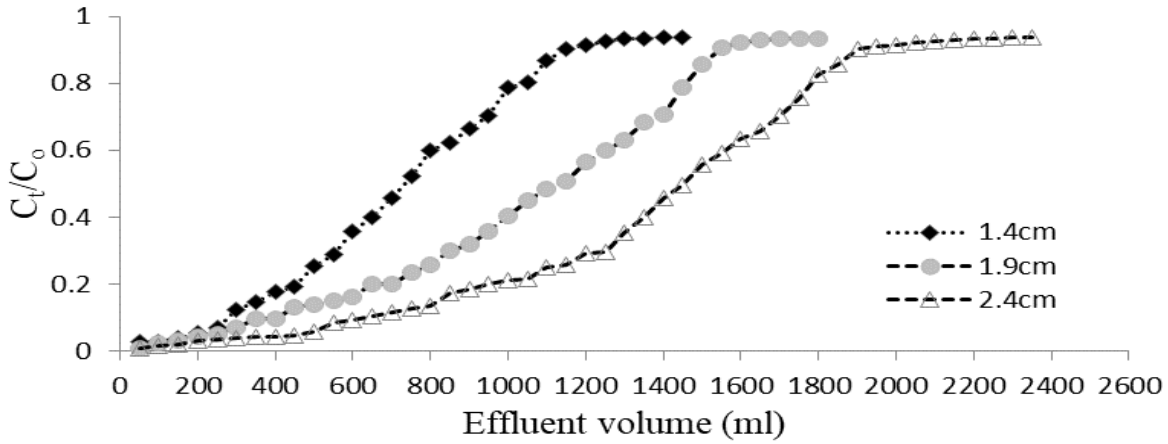


**Figure 3:** Effects of bed depth on sorption of BG on clay bound AMLP (CAMLP) at 303K (flow rate 1.5mL$min^{-1}$, BG concentration 20 $mgL^{-1}$).

It is observed that as the feed concentration increased from 10 to 30 mg $L^{-1}$ of both dyes (MB and BG) in single system, breakthrough volume decreases, i.e. for 90% breakthrough of MB, breakthrough volume decreases from 2.20 to 1.05 L and 2.00 to 0.95 L for BG. Similarly, for 50% breakthrough, MB breakthrough volume decreases from 1.50 to 0.55L and BG from 1.50 to 0.50L (Table 3). However, adsorption capacities increase with increase in feed concentration and this may be attributed to the fact that at higher concentration the driving force for mass transfer was increased saturating the adsorbent more quickly with increase in feed concentrations which in turn increases the adsorption capacity for MB from 2.61 to 5.10 mg $g^{-1}$ (for 90% breakthrough) and 1.37 to 3.48 mg $g^{-1}$ (for 50% breakthrough). Similar results were also observed for increase of feed concentrations of BG, adsorption capacity increased from 1.25 to 3.90 mg $g^{-1}$ (for 90% breakthrough) and from 2.38 to 5.20 $mgg^{-1}$(for 50% breakthrough). Therefore, it can be concluded that the adsorption process is concentration dependent [18]. Similar results have also been obtained by Ansari et al. (2011) for adsorption of MB on unripe grape waste at feed concentration of 40 to 100 mg $L^{-1}$.

**Table 2-** The column adsorption capacities of clay bound biosorbents at 50% and 90% breakthrough points for three different bed depth 1.4, 1.9 and 2.4 cm for fixed feed dye concentration, 20ppm and constant flow rate, 1.5 $mLmin^{-1}$ at 303K (BV=Breakthrough Volume Adv cap=adsorptions capacities)

| Sorbents | Flow rate ($mlmin^{-1}$) | | Bed Depth (cm) | 90% breakthrough | | | 50% Breakthrough | | |
|---|---|---|---|---|---|---|---|---|---|
| | | | | BV (L) | Time (h) | Ad Cap ($mgg^{-1}$) | BV (L) | Time (h) | Ad Cap ($mgg^{-1}$) |
| CAMLP | MB | 1.5 | 1.4 | 1.00 | 11.11 | 2.30 | 0.50 | 5.56 | 1.15 |
| | | | 1.9 | 1.70 | 18.89 | 3.05 | 1.15 | 12.78 | 2.06 |
| | | | 2.4 | 2.45 | 27.22 | 3.55 | 2.00 | 22.22 | 2.90 |
| | BG | 1.5 | 1.4 | 1.15 | 12.78 | 2.85 | 0.75 | 8.33 | 1.24 |
| | | | 1.9 | 1.55 | 17.22 | 2.86 | 1.15 | 12.78 | 2.10 |
| | | | 2.4 | 1.90 | 21.11 | 2.99 | 1.45 | 16.11 | 2.90 |

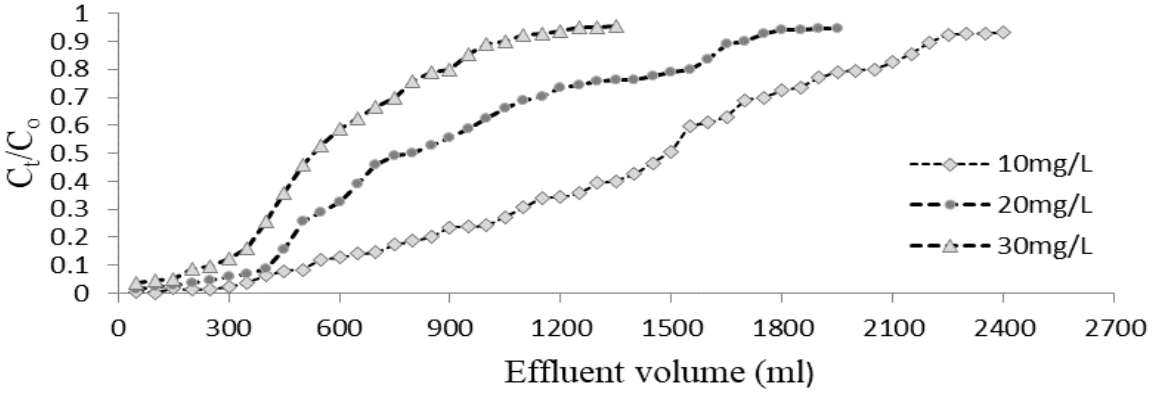


**Figure 4.** Effects of feed concentration on adsorption of MB on clay bound AMLP (CAMLP) at 303 K (bed depth 1.4 cm, flow rate 1.5$mLmin^{-1}$).

### 3.2.3 Effect of flow rate

In order to investigate the effect of flow rate on breakthrough at 90 % and 50% at constant bed depth (1.4 cm) and feed concentration of both dye (20 mg $L^{-1}$), the dye solutions were allowed to flow through the sorbent bed at three different flow rates such as 1.5, 3.7- and 5.2-mL $min^{-1}$. The breakthrough curves plotted are shown in Figure 6 for MB and Figure 7 for BG.

**Table 3-** The column adsorption capacities of CAMLP at 50% and 90% breakthrough points at three different feed concentrations 10, 20 and 30 $mgL^{-1}$ for fixed flow rate, 1.5$mLmin^{-1}$ and bed depth, 1.4cm at 303K (BV=Breakthrough Volume, Adv cap=adsorptions capacities).

| Sorbents | Flow rate (mL/min) | | Dye concentration ($mgL^{-1}$) | 90 % breakthrough | | | 50 % Breakthrough | | |
|---|---|---|---|---|---|---|---|---|---|
| | | | | BV (L) | Time (h) | Ad Cap ($mgg^{-1}$) | BV (L) | Time (h) | Ad Cap ($mgg^{-1}$) |
| CAMLP | MB | 1.5 | 10 | 2.20 | 24.45 | 2.61 | 1.50 | 16.67 | 1.37 |
| | | | 20 | 1.70 | 18.89 | 3.91 | 0.80 | 8.89 | 1.84 |
| | | | 30 | 1.05 | 11.67 | 5.10 | 0.55 | 6.11 | 3.48 |
| | BG | 1.5 | 10 | 2.00 | 22.22 | 1.25 | 1.50 | 16.67 | 2.38 |
| | | | 20 | 1.50 | 16.67 | 2.60 | 1.05 | 11.67 | 3.71 |
| | | | 30 | 0.95 | 10.56 | 3.90 | 0.50 | 5.56 | 5.20 |

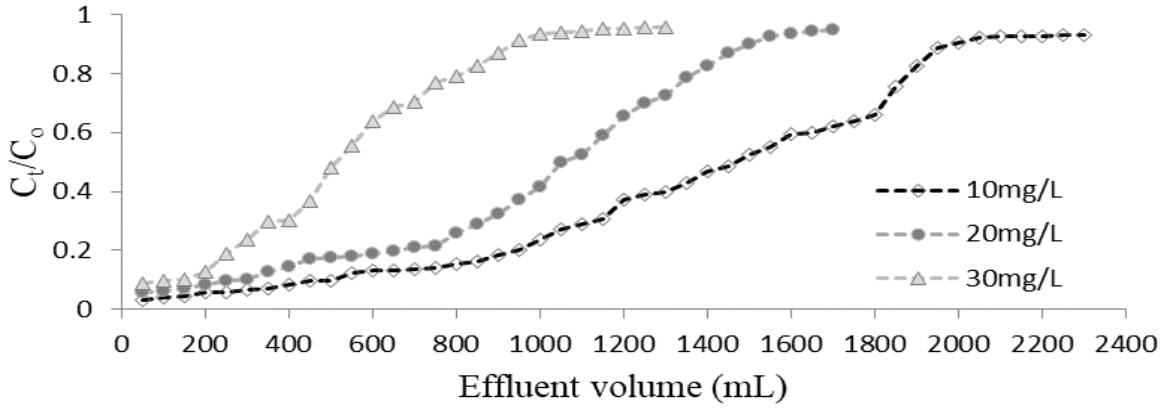


**Figure 5:** Effects of feed concentration on adsorption of BG on clay bound AMLP (CAMLP) at 303 K (bed depth 1.4 cm, flow rate 1.5mLmin$^{-1}$).

It was seen from the figure Figure. 6 and 7 that as the flow rate increases from 1.5 to 5.2 mLmin$^{-1}$; the breakthrough curve becomes steeper, indicating quick saturation of the sorbent bed. It might be due to at higher adsorbate flow rate, dye molecule/ion of MB and BG had less time to contact with the clay bound AMLP bed which resulted into steeper breakthrough curve (Table 4). Moreover, at higher flow rate, the rate of mass transfer increase leading to faster saturation of sorbent bed [12]. Further with increase in flow rate all the three parameters i.e. breakthrough time, breakthrough volume and adsorption capacity decreases.

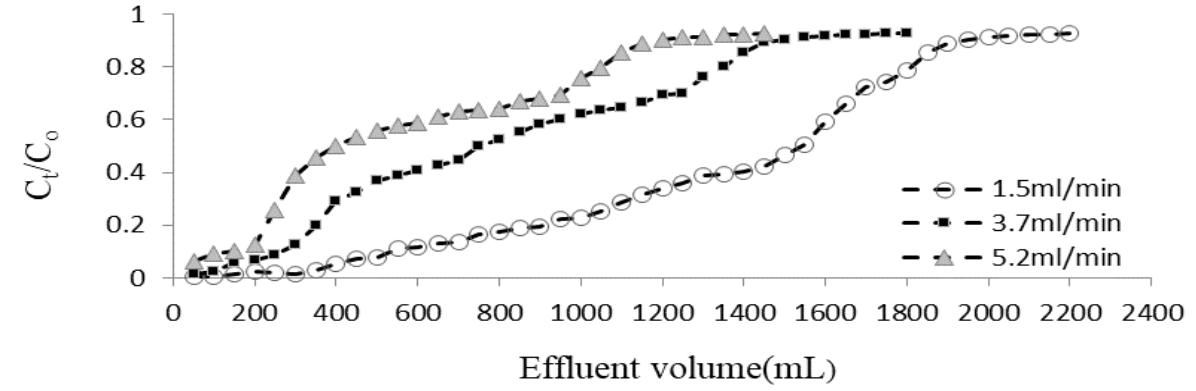


**Figure 6:** Effects of flow rate on adsorption of MB on clay bound AMLP (CAMLP) at 303 K (bed depth 1.4cm, MB concentration 20mgL$^{-1}$).

For 90% breakthrough, the breakthrough time decreases from 21.67 to 3.85 h, breakthrough volume from 1.95 to 1.2 L and adsorption capacity from 4.49 to 2.75 mg g$^{-1}$ for MB adsorption on CAMLP. Similarly, for 50% breakthrough, breakthrough time decreases from17.22 to 1.28 h, breakthrough volume from 1.5 to 0.4 L and adsorption capacity from 3.57 to 0.92 mg g$^{-1}$ for MB adsorption on CAMLP.

In case of BG adsorption on CAMLP, with increase in flow rate, breakthrough time decreases from 25 to 3.21 h, volume from 2.25 to 1.0 L and adsorption capacity from 5.57 to 2.42 mg g$^{-1}$ for 90 % breakthrough and for 50% breakthrough, breakthrough time decreases from 16.67 to 2.25 h, volume from 1.5 to 0.7 L and adsorption capacity from 3.71 to 1.68 mg g$^{-1}$ respectively.

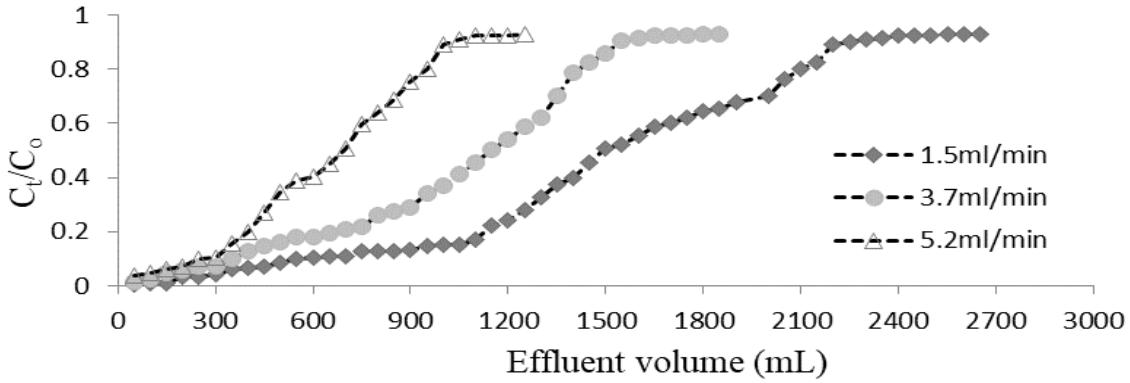


**Figure 7:** Effects of flow rate on adsorption of BG on clay bound AMLP(CAMLP) at 303 K (bed depth 1.4cm, BG concentration 20mgL$^{-1}$).

This is because at lower flow rate, interactions between the adsorbent and adsorbate ions had ample time, resulting in a higher dye sorption capacity [19]. Similar results have been reported by [20] in their adsorption studies on the removal of MB from aqueous solution using coconut husk as an adsorbent. They have reported that the MB adsorption per unit adsorbent mass decreased slightly with increasing the flow rate at the same bed depth.

**Table 4-** The column sorption capacities of clay bound AMLP at 50% and 90% breakthrough points at three different flow rates 1.5, 3.7 and 5.2-mL min$^{-1}$ for fixed feed concentration, 20 mgL$^{-1}$ and bed depth, 1.4 cm at 303 K.

| Sorbents | Bed depth(cm) | | Flow rate mLmin$^{-1}$ | 90% breakthrough | | | 50% Breakthrough | | |
|---|---|---|---|---|---|---|---|---|---|
| | | | | BV (L) | Time (h) | Ad Cap (mgg$^{-1}$) | BV (L) | Time (h) | Ad Cap (mgg$^{-1}$) |
| CAMLP | MB | 1.4 | 1.5 | 1.95 | 21.67 | 4.49 | 1.55 | 17.22 | 3.57 |
| | | | 3.7 | 1.50 | 06.76 | 3.48 | 0.75 | 03.38 | 1.74 |
| | | | 5.2 | 1.20 | 03.85 | 2.75 | 0.40 | 01.28 | 0.92 |
| | BG | 1.4 | 1.5 | 2.25 | 25.00 | 5.57 | 1.50 | 16.67 | 3.71 |
| | | | 3.7 | 1.55 | 06.98 | 3.17 | 1.15 | 05.18 | 2.35 |
| | | | 5.2 | 1.00 | 03.21 | 2.42 | 0.70 | 02.25 | 1.68 |

### 3.2.4 The Bohart-Adam's model

The BDST (Bed Depth Service Time) model is used to describe and prediction of the dynamic behaviours of the clay-bound biosorbent (CAMLP) beds in column performance. The BDST plots were obtained by plotting service time (min) against bed depth for CAMLP for three different bed heights 1.4 cm, 1.9 cm, and 2.4 cm at breakthrough concentration of 20%, 40%, 60% and 80% are shown in Figure. 8 and Figure. 9. The parameters of Bohart – Adam's model for the sorption of MB and BG on CAMLP were obtained from the slope and intercept of these plots and are given in Table 5 and Table 6 respectively.

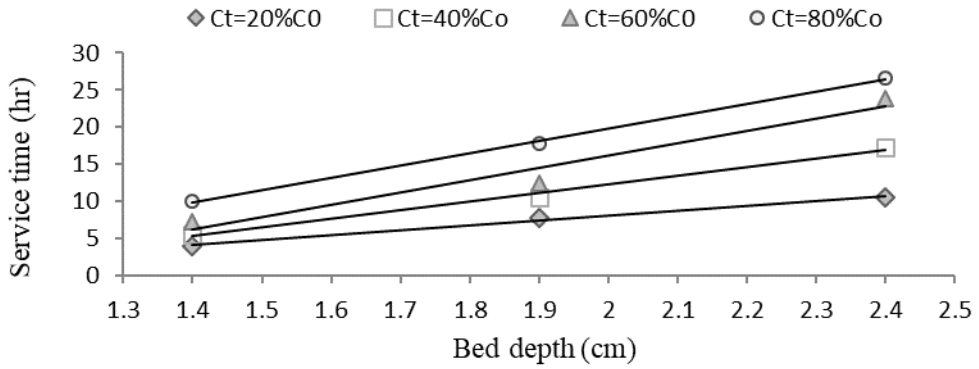


**Figure 8:** Bohart-Adam's model plots for adsorption of MB on CAMLP at constant flow rate 1.5 mLmin-1, MB concentration 20 mgL-1and at 303K.

It is observed that the adsorption capacity ($N_o$) value for both dye increases from 20% to 80%, which indicates that with time the column becomes saturated with dye ions and the adsorption sites on the bed becomes less available for both the dye ions [21]. However, the mass transfer co-efficient $K_{AB}$ decreases from 0.14 to 0.13 $Lg^{-1}h^{-1}$, 0.24 to 0.17 $Lg^{-1}h^{-1}$, -0.001 to -0.002 $Lg^{-1}h^{-1}$ and -0.005 to -0.006 $Lg^{-1}h^{-1}$, for MB–CAMLP with increase in bed depth from 1.4 cm to 2.4 cm as the breakthrough value rises from 20 to 80%. Similarly, for BG-CAMLP sorption system, $K_{AB}$ values decreases from 0.024 to 0.023 $Lg^{-1}h^{-1}$, 0.006 to 0.005 $Lg^{-1}h^{-1}$, -0.0074 to -0.008 $Lg^{-1}h^{-1}$ and 0.701 to 0.565 $Lg^{-1}h^{-1}$ as the breakthrough value rises from 20 to 80%. This showed that the overall kinetics was dominated by external mass transfer [22].

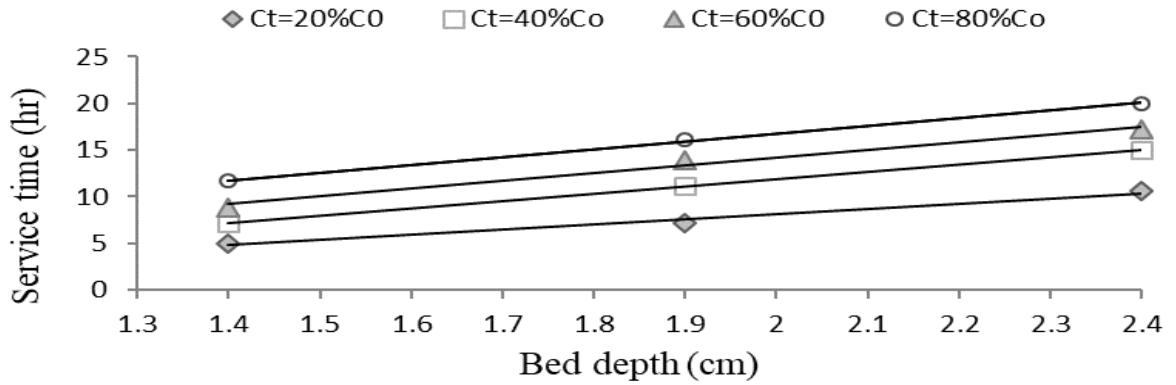


**Figure 9:** Bohart-Adam's model plots for adsorption of BG on CAMLP at constant flow rate 1.5 mLmin-1, BG concentration20 mgL-1and at 303K.

**Table 5-** Bohart-Adam's model parameters for column sorption of MB on CAMLP.

| Breakthrough point (%) | Slope | Intercept | Adsorption Capacity, No($gL^{-1}$) | Bed-Depth (cm) | $K_{AB}$ ($Lg^{-1}h^{-1}$) | Regression Coefficient (R) |
|---|---|---|---|---|---|---|
| 20 | 6.667 | -5.259 | 0.226 | 1.4 | 0.014 | 0.995 |
| | | | | 1.9 | 0.013 | |
| | | | | 2.4 | 0.013 | |
| 40 | 11.66 | -11.05 | 0.396 | 1.4 | 0.0024 | 0.996 |
| | | | | 1.9 | 0.0019 | |
| | | | | 2.4 | 0.0017 | |
| 60 | 16.66 | -17.13 | 0.566 | 1.4 | -0.0011 | 0.921 |
| | | | | 1.9 | -0.0012 | |
| | | | | 2.4 | -0.002 | |
| 80 | 16.66 | -13.51 | 0.566 | 1.4 | -0.005 | 0.999 |
| | | | | 1.9 | -0.0051 | |
| | | | | 2.4 | -0.006 | |

**Table 6-** Bohart-Adam's model parameters for the column sorption of BG CAMLP.

| Breakthrough point(%) | Slope | Intercept | Adsorption Capacity, No($gL^{-1}$) | Bed-Depth (cm) | $K_{AB}$ ($Lg^{-1}h^{-1}$) | Regression Co-efficient(R) |
|---|---|---|---|---|---|---|
| 20 | 5.56 | -2.963 | 0.166 | 1.4 | 0.024 | 0.993 |
| | | | | 1.9 | 0.023 | |
| | | | | 2.4 | 0.022 | |
| 40 | 7.78 | -3.667 | 0.233 | 1.4 | 0.006 | 0.100 |
| | | | | 1.9 | 0.005 | |
| | | | | 2.4 | 0.005 | |
| 60 | 8.33 | -2.501 | 0.249 | 1.4 | -0.0074 | 0.993 |
| | | | | 1.9 | -0.008 | |
| | | | | 2.4 | -0.008 | |
| 80 | 8.33 | 0.100 | 0.250 | 1.4 | 0.701 | 0.999 |
| | | | | 1.9 | 0.660 | |
| | | | | 2.4 | 0.565 | |

A high value of regression coefficient was obtained when these predicted values of breakthrough time were plotted against the observed values of breakthrough time. The regression co-efficient values for both dyes are comparatively high i.e. ($0.995 < R < 0.999$) for MB and ($0.993 < R < 1$) for BG which supports the applicability of Bohart-Adam's model for the adsorption of MB and BG onto CAMLP column.

**3.2.5 Desorption and regeneration of column**

In the present work, dilute NaOH was selected as the eleunt for desorption process and it is seen that 0.1N NaOH is efficient in removing both MB and BG from clay bound AMLP biosorbents and it is likely that ion exchange type of interaction exists between the dye ions and the sorbents surface [23]. Karthik et al., (2015) [24] has successfully used 1% NaOH in the desorption of MB from saw dust, almost 98.2% is desorbed, banana fibre desorbed about 86.7% and coconut fibre desorbed the dye by 12.4%. Pathania et al., (2017) [25] has successfully desorbed MB from FCBAC surface by using NaOH as eluent.

Desorption experiment was carried out on two columns having bed depth 1.9 cm of CAMLP and each column was saturated with 20 $mgL^{-1}$ MB and BG at flow rate 3.7 mL $min^{-1}$. The desorption curves for MB and BG are shown in Fig. 10 and Fig. 11 respectively It is observed that about 8.56 h was required to saturate the column of CAMLP with 1.9 L of MB and about 8.78 h required to saturate with 1.95 L of BG. The 1.9 cm bed depth column contains 11.15 g of CAMLP. The granulated clay bound (CAMLP) biosorbent has adsorption capacity was found 3.41 mg $g^{-1}$ for MB and 3.32 $mgg^{-1}$ for BG. Thereafter, the adsorbed MB and BG ions were eluted from the column by using 0.1 N NaOH as the eluent at a constant flow rate of 2.3 mL $min^{-1}$, this flow rate is less that the adsorption flow rate of 3.7 mL $min^{-1}$.

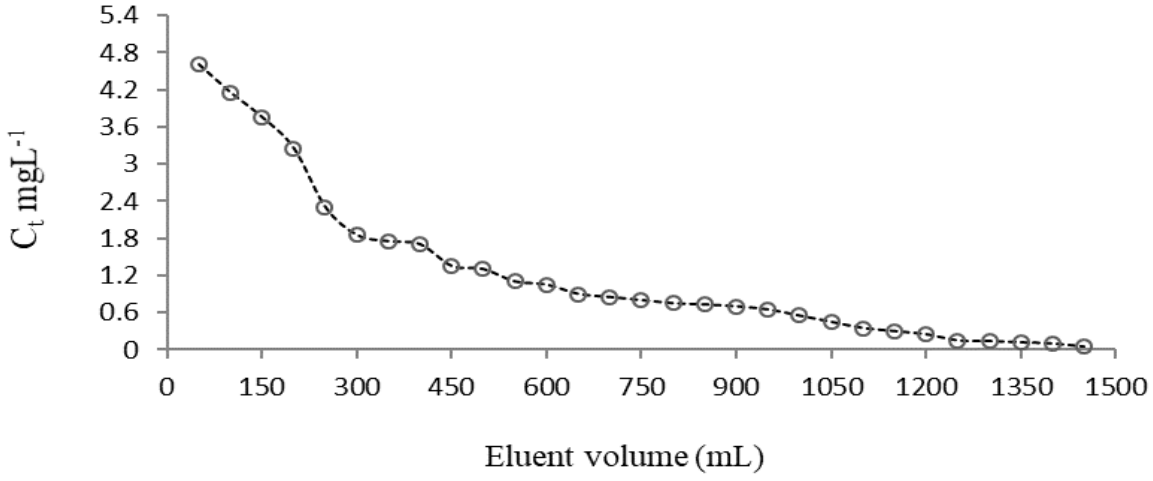


**Figure 10:** Desorption of methylene blue (MB) from MB-loaded CAMLP column at 303 K with aqueous0.1 N NaOH (bed depth 1.4 cm, flow rate 2.3 mLmin-1).

The desorption curves for both MB and BG removal from dye loaded CAMLP column are shown in Fig 12 and Fig 13 respectively. For desorption of MB, 1.45 L of 0.1N NaOH solution required and time for exhaustion was found to be 10.51 hrs. For BG, 1.30L of 0.1N NaOH solution was required and time for exhaustion was 9.42 hrs. The desorption capacity of 1.0 g of CAMLP, 2.60 mg for MB and 2.33 mg for BG. It was observed that about 76% of MB and 67% of BG had been desorbed from the dye adsorbed CAMLP using 0.1N NaOH solution.

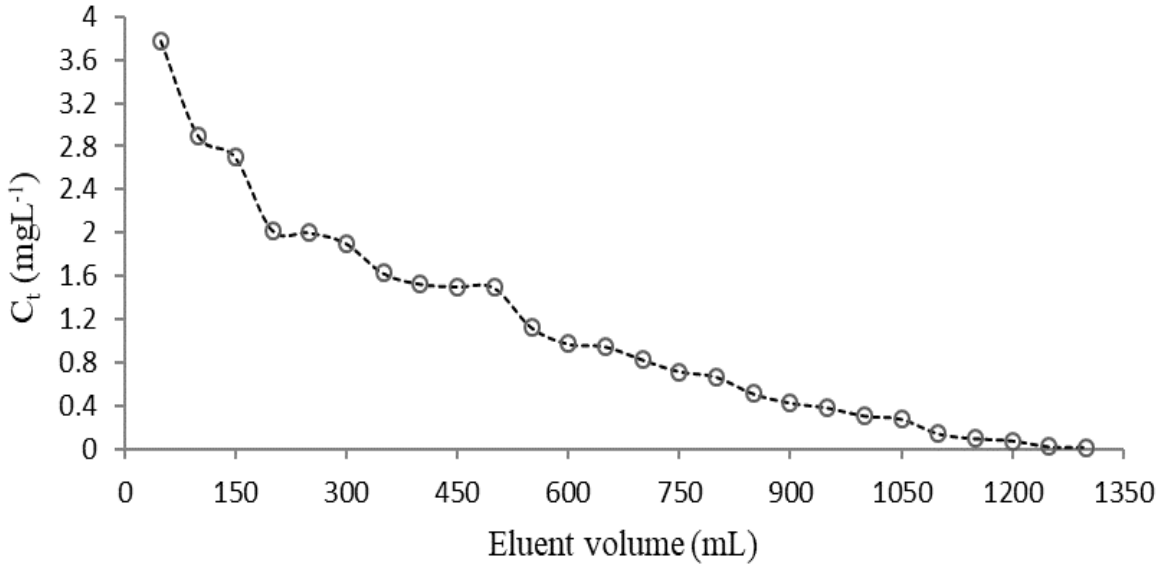


**Figure 11:** Desorption of brilliant green (BG) from BG-loaded CAMLP column at 303K with aqueous0.1 N NaOH (bed depth 1.4 cm, flow rate 2.3 mLmin-1).

From the experimental results it was observed that adsorption efficiency of CAMLP was higher in case of BG than MB (BG > MB) but in case of desorption efficiency CAMLP is more favourable for MB than BG (MB > BG). This may be due to the structure of the dyes that influence the dye molecule/ion interactions with the sorbents in aqueous phase.

## IV. CONCLUSIONS

Adsorption capacities of the clay bound biosorbents i.e. CAMLP increases with the increase in bed depth from 1.4cm to 2.4cm keeping the feed concentration (20mgL-1) of both MB and BG for single system constant and flow rate (1.5 mLmin-1) constant. Increasing the feed concentration from 10 to 30mgL-1 for both MB and BG in single system but keeping both bed depth (1.4 cm) and flow rate (1.5 mLmin-1) constant, adsorption capacities of the biosorbents increases with increasing the feed concentration. When the flow rate of feed solution was varied from 1.5 to 5.2 mLmin-1 but the bed depth (1.4 cm) and the feed concentration (20mgL-1) were kept constant, both MB and BG adsorption capacity of the clay bound biosorbents, CAMLP decreased with increasing flow rate. The Bohart Adam's model could be successfully applied to both MB and BG adsorption by CAMLP in the dynamic column adsorption process. Desorption of both MB and BG adsorbed adsorbent bed was successfully carried using 0.1N NaOH solution and almost 76% of MB and 67% of BG had been desorbed from CAMLP and thus the adsorbent bed is regenerated.

## ACKNOWLEDGEMENT

I want to acknowledge Department of Science and Technology (DST)/Water Technology Initiative(WTI) Programme, India for their financial support throughout this work

## REFERENCES

[1]. Ho Y.S., McKay G., (1998). "Sorption of dye from aqueous solution by peat", Chem. Eng. J, Vol. 72 (2), pp. 115–124.
[2]. Padmesh T.V.N., Vijayaraghavan K., Sekaran G., Velan M., (2005). "Batch and column studies on biosorption of acid dyes on fresh water macro alga", J. of Hazardous Mater., Vol. 125 (1-3), pp 121-129.
[3]. Fu Y. and Viraraghavan T., (2001). "Fungal decolorization of dye wastewaters: a review", Bioresour. Technol, Vol. 79, pp 251–262.

[4]. Zhang W., Li H., Kan X., Dong L., Jiang Z., Yang H and Cheng R. (2012). "Adsorption of anionic dyes from aqueous solutions using chemically modified straw", Bioresource Technology, Vol. 117, pp. 40–47.
[5]. Kabbout R., Taha S. (2014). "Biodecolorization of textile dye effluent by biosorption of fungal biomass materials",Physics Procedia., Vol. 55, pp 437-444.
[6]. Kaushik P., Malik A., (2009). "Fungal dye decolourization: Recent advances and future potential", Environ. Internat, Vol. 35(1), pp 127-141.
[7]. Ho Y.S., McKay G., (2003). "Sorption of dyes and copper ions onto biosorbents. Process Biochem", Vol. 38, pp 1047– 1061.
[8]. Maghraby A.E and Deeb H.A. (2011). "Removal of a basic dye from aqueous solution by adsorption using rice hull", Global NEST Journal, Vol.13, pp.90-98.
[9]. Weber W. J. Jr. (1972). "Physiochemical Process for Water Quality Control". Willey Interscience, New York. 640.
[10]. Pirajana J.C.M., Rangel D., Amaya B., Vargas E.M and Giraldo L. (2008). Design and construction of equipment to make adsorption at pilot plant scale of heavy metals. Z. Naturforsch, Vol. 63, pp.453 – 461.
[11]. Tofan L., Paduraru C., Teodosiu C and Toma O. (2015). "Fixed bed column study on the removal of chromium (III) ions from aqueous solutions by using hemp fibers with improved sorption performance", Cellulose Chem. Technol, Vol. 49(2), pp. 219-229.
[12]. Dutta M., Basu J.K., Md Faraz H., Gautam N and Kumar A. (2012). Fixed-bed Column Study of Textile Dye Direct Blue 86 by using A Composite Adsorbent. Archives of Applied Science Researc, Vol. 4 (2), pp. 882-891.
[13]. Zhanying Z., Ian O., Geoff A.K and William O.S.D. (2013). "Comparative study on adsorption of two cationic dyes by milled sugarcane bagasse", Industrial Crops and Products, Vol. 42, pp. 41-49.
[14]. Chakravarty S., Mohanty A., Sudha T.N., Upadhyay A.K., Konar J., Sircar J.K., Madhukar A and Gupta K.K. (2010). "Removal of Pb (II) ions from aqueous solution by adsorption using bael leaves (Aegle marmelos)", Journal of Hazardous materials, Vol.173, pp.502-509.
[15]. Ahmad R., Kumar R and Haseeb S. (2010). "Adsorption of $Cu^{2+}$ from aqueous solution onto iron oxide coated eggshell powder: Evaluation of equilibrium, isotherm, kinetics and regeneration capacity", Arabian Journal of Chemistry, Vol.48, pp. 3051-3057.
[16]. Vijayaraghavan K., Jegen J., Palanivelu K and Velan M. (2004). "Removal of nickel (II) ions from aqueous solution using crab shell particles in a pact bed up – flow column", Journal of hazardous materials, Vol. 113 (1-3), pp. 223-230.
[17]. Sharma S.K., Peter A and Obot I.B. (2015). "Potential of Azadirachata indica as a green corrosion inhibitor against mild steel, aluminium and tin: a review", Journal of Analytical Science and Technology, Vol.6:26, pp.1-26.
[18]. Goel J., Kadirvelu K., Rajagopal C and Garg V.K. (2005). "Removal of lead (II) by adsorption using treated granular activated carbon: Batch and column studies", Journal of Hazardous Material, Vol.125(1-3), pp.11-20.
[19]. Kamal S., Manmohan S and Birendra S. (2010). "A review on chemical and medicobiological application of *Jathropha Curcas"*, International Research Journey of pharmacy, Vol. 2(4), pp.61-66.
[20]. Hasfalina C.B.M., Christopher O.A and Jun C.X. (2015). "Coconut husk adsorbentfor the removal of methylene blue dye from waste water", Bioresources, Vol. 10(2), pp. 2859-2872.
[21]. Chen N., Zhang Z., Feng C., Li M., Chen R and Sugiura N. (2011). "Investigations on batch and fixed bed column performance of fluoride adsorption by Kanuma mud", Desalination, Vol. 268, pp.76-82.
[22]. Han R., Wang Y., Zhao X., Wang Y., Xie F., Cheng J and Tang M. (2009). "Adsorption of methylene blue by phoenix tree leaf powder in a fixed-bed column: experiments and prediction of breakthrough curves", Desalination, Vol. 245, pp. 284–297.
[23]. Yan C and Liu X. (2009). "Adsorption of methylene blue on mesoporous carbon prepared using acid and alkaline treated Zeolite X as the template", Colloids and surfaces A: physicochemical and Engineering Aspects, Vol.333(1-3), pp.115-119.
[24]. Karthik R., Pushpam A.C., Vanitha M.C and Rekha V. (2015). "Elimination of methylene blue from aqueous solution using biosorbents under stirring and stagnant conditions", International Journal of Advanced Research in Engineering and Technology (IJARET), Vol.6 (10), pp. 76-85.
[25]. Pathania D., Sharma S and Singh P. (2017). "Removal of methylene blue by adsorption ontoactivated carbon developed from Ficus carica bast", Arabian Journal of Chemistry, Vol. 10, pp. 1445–1451.

Smita Baruah, et. al. "Efficiency of a biosorbent from Aegle marmelos leaves for removal of MB and BG from aqueous solution using column method." *Quest Journals Journal of Research in Environmental and Earth Science*, vol. 06, no. 04, 2020, pp. 34-47.